

# Time-stepped exergy analysis, environmental and economic evaluation of a new designed natural ventilation system

Onur Kayapinar, Oğuz Arslan\*

Department of Mechanical Engineering, Bilecik Şeyh Edebali University, Bilecik, Turkey

## ARTICLE INFO

### Keywords:

Time-stepped exergy analysis  
Experimental investigation  
Industrial buildings  
Natural ventilation system design  
Net present value

## ABSTRACT

This study investigates a new stack-type natural ventilation system (NVS) designed for small and medium-scaled industrial buildings. The NVS was designed and constructed for the disposal of the welding gases to obtain suitable working conditions from the thermal comfort point of view. The NVS system was analyzed by time stepped exergy analysis based on experimental data observed for a yearlong measurement. The experimental set-up was established to determine the ventilation throughout the wind speed measurements, temperature, and relative humidity measurements. Besides, the NVS was economically evaluated by the net present value (NPV) method. The exergy efficiency of the system was recorded ranging between 65 and 95% depending on the external conditions such as wind speed and outdoor temperature. With annual ventilation of  $6,850.80 \text{ m}^3/\text{h}$ , it was determined that an annual saving of  $12,092.20 \text{ m}^3$  of natural gas, 1045.11 tones of  $\text{CO}_2$  emission, and 0.0345 GWh electricity was available. The system was found investable with an NPV of 18,576.61 \$ for a lifetime of 20 years.

## Introduction

Industrial buildings are increasing day by day as a result of the development of the industry and the increase in the need for production. The most crucial need of industrial production is the necessary infrastructure conditions. Disposal of harmful gases that result from production processes is one of these necessities since it directly affects employee comfort and health. So, ventilation systems to increase indoor air quality are inevitable. Since the application and operation of air conditioning systems for industrial buildings are relatively expensive, these systems are not preferred in small and medium-scale industrial buildings.

Several natural ventilation strategies such as single-sided, cross, wind tower, solar chimney, atrium, and stack ventilation were reported [1]. There are two main driving forces in all these kinds of strategies: thermal buoyancy- and wind-induced. Thermal buoyancy-induced ventilation occurs by the differential pressure sourced by the temperature difference between the indoor and outdoor. The wind-induced ventilation occurs by the differential pressure sourced by the pressure drop at the ventilation cross-section due to the wind velocity [2–4]. Under the actual conditions of a building, the coupled effects of these two terms exist [5]. Also, the climatic conditions of the location of the

ventilated building are an essential parameter that determines the performance of the NVS. Li and Chen [6] determined five climatic zones, namely severe cold areas (zone 1), cold areas (zone 2), hot summer and cold winter areas (zone 3), hot summer and warm winter areas (zone 4), moderate areas (zone 5), depending on the winter and summer conditions in their study. They concluded that Zone 5 has the most considerable financial savings and cooling potential, whereas Zone 1 was recommended as the first for seasonal ventilation strategies.

In this context, natural ventilation systems (NVSs) are an energy and cost-efficient ventilation strategy. Many studies about the NVS applied to several building types exist in the literature. Espinoza et al. [7] analyzed the impact of the ventilator configuration on the internal airflow pattern in a three-span Mediterranean greenhouse. The results show that the airflow pattern in the greenhouse depends on the distribution of the ventilation surface and the ventilation obstruction. The study conducts that the double-sided ventilation system improves airflow patterns. Hulsure and Maurya [8] conducted a numerical analysis of the application of an NVS for an industrial warehouse building with a length of 145 m, a width of 75 m, and a height of 6 m. It was concluded that an NVS installed on the roof ridge increased the ventilation rate by 8%. Gil-Baez et al. [9] investigated experimentally and numerically the indoor air quality parameters and energy use for the NVS located on the school buildings under mild climate conditions. A

\* Corresponding author.

E-mail address: [oguz.arslan@bilecik.edu.tr](mailto:oguz.arslan@bilecik.edu.tr) (O. Arslan).

<https://doi.org/10.1016/j.tsep.2023.102058>

Received 19 May 2023; Received in revised form 24 June 2023; Accepted 10 August 2023

Available online 14 August 2023

2451-9049/© 2023 Elsevier Ltd. All rights reserved.

Nomenclature	
<i>A</i>	Area (m <sup>2</sup> )
<i>E</i>	Energy, Exergy (Kj/h)
<i>C</i>	Cost (\$)
<i>C<sub>d</sub></i>	Discharge coefficient
<i>P</i>	Pressure (Pa)
<i>T</i>	Temperature (°C)
<i>V</i>	Volume (m <sup>3</sup> )
<i>Q</i>	Flow (m <sup>3</sup> /s)
<i>h</i>	Height (m)
<i>A</i>	Area (m <sup>2</sup> )
<i>U</i>	Uncertainty
<i>f</i>	Unit price (\$)
<i>X</i>	Observations
<i>R</i>	Universal gas constant (kJ/kmol K)
<i>N</i>	Number of NVS unit
<i>Greek Letter</i>	
<i>ρ</i>	density (kg/m <sup>3</sup> )
<i>n</i>	Number of units
*	Average value, per kmole -fuel
<i>φ</i>	Humidity of air (%)
<i>ε</i>	Efficiency (%)
<i>v</i>	Speed (m/s)
<i>ω</i>	Specific Humidity Ratio
<i>Subscripts</i>	
<i>a</i>	Air
<i>atm</i>	Atmosphere
<i>building</i>	Building
<i>da</i>	Dry air
<i>cf</i>	Cash flow
<i>e</i>	Electricity
<i>ec</i>	Electric consumption
<i>in</i>	Inside
<i>out</i>	Outside
<i>L</i>	Labor or Loss
<i>m</i>	Moisture, measurement, mass
<i>ng</i>	Natural gas
<i>r</i>	Speed of wind or discount rate
<i>p</i>	Piping
<i>ph</i>	Physical
<i>s</i>	Saturated
<i>st</i>	Sheet metal
<i>sys</i>	System
<i>t</i>	Number of measurement
<i>te</i>	Natural gas turbine engine
<i>w</i>	Welding
<i>ws</i>	Welding supply
<i>x</i>	Exergy
<i>wm</i>	Water moisture
<i>wo</i>	Worker
<i>Abbreviations</i>	
<i>NPV</i>	Net present value
<i>NVS</i>	Natural ventilation system
<i>SD</i>	Standard deviation

primary energy saving of about 18–33% was reported to supply the required indoor environmental quality (IEQ) norms in the study. Mukhtar et al. [10] investigated the design strategies of the NVSs in underground buildings. They indicated that there are limited passive designs to improve thermal comfort and reduce energy consumption under the required IEQ. Dorizas et al. [11] investigated the performance of the NVS for a school building experimentally. They indicated that external conditions, such as wind speed, significantly affect the system's operational performance. Su et al. [12] established an evaluation method based on thermal comfort for testing the NVS. With this aim, they investigated an office building equipped with a single NVS. They conducted that the system is enough to obtain the basic requirements of the thermal comfort conditions. Shi et al. [13] investigated the green roof and natural ventilation systems for office buildings. They indicated that the optimal design could save energy by 12.2%. Chen et al. [14] proposed a control strategy based on the prediction of an hour-head model for natural ventilation systems in passive buildings. In comparison to the traditional control strategy, they reported an increase in the ventilation rate by 56.3% via a data-driven prediction model. In the study, they aimed to maximize natural ventilation to achieve near-zero energy consumption. Gilvaei et al. [15] investigated a novel passive system for the natural ventilation of a building. They aimed to reduce the energy consumption of the mechanical ventilation system by hybridizing a wind-catcher, a heat exchanger, and an evaporative cooling system in a residential building. They reported an electricity saving of 0.0194 kWh/m<sup>2</sup> in comparison to the split air conditioner. Shaeri et al. [16] proposed a new wind chimney for the natural ventilation of coastal buildings. They reported an increase of 117.9% in the ventilation rate compared to the building without the wind chimney. Tognon et al. [17] investigated the hybrid ventilation control systems for different building types and climates. They reported that it was available to reduce the sensible heat by up to 31%, latent heat by up to 30%, and fan

absorptions by up to 86%. Xie et al. [18] investigated the effects of locations of rural residential buildings on natural ventilation. They reported that hilly terrains and the distance between the buildings as well as the winter and summer conditions affects the natural ventilation. Li et al. [19] investigated the night ventilation schemes for mechanical and natural ventilated buildings. They reported that it was available to reduce energy consumption by up to 15.29% through natural ventilation. He et al. [20] investigated the efficiency enhancement of natural ventilation by the roof window in an active house building. They reported that the ventilation efficiency enhancement by the roof window was 1.62 times higher than the mechanical ventilation. Song et al. [21] investigated the effects of window openings at different heights on natural ventilation. They indicated that cross ventilation with stack effects was the most efficient natural ventilation mode. They reported that it was available to save energy by 5.6 kWh/m<sup>2</sup> for the optimal natural ventilation mode. Ma'bdeh et al. [22] investigated the different natural ventilation retrofitting for a classroom. Solar chimney assisting a wind tower was determined as the best natural ventilation technique. By this system, it was reported that it was available to achieve an energy saving of 39% in comparison to a split air condition system.

Although natural (or passive) ventilation is commonly used wittingly or unwittingly in all buildings; it is vital to design the NVS for adequate ventilation in industrial buildings. In this study, a new stack-type NVS was designed for a medium-scale industrial building. By this new NVS, it was aimed to obtain zero energy consumption as well as the disposal of the non-breathable gases resulting from the production processes for suitable working conditions. An experimental set-up was established to determine the ventilation throughout the wind speed measurements, temperature, and relative humidity measurements. The experiments were recorded on an hourly basis for one year. Accordingly, time stepped exergy analysis based on the hourly data was conducted to determine the performance of the NVS for the first time. So, the exergy

destructions were determined to observe the effects of entropy generation on the environment since the destruction gives the entropy generation that causes global warming. The emission and energy savings were later determined for the regional conditions. Finally, the system was evaluated economically through the net present value (NPV) method considering the required NVS for current labor conditions.

**Material and method**

*Study area*

The designed NVS was installed in small-scale industrial buildings with welding and non-welding manufacturing methods. With this new design, it was aimed to obtain thermal comfort conditions by the removal of welding wastes that reduce employee comfort. The building is located in Bozuyuk industrial estate in hot summer and cold winter conditions (zone 3). The building has a volume ( $V_{building}$ ) of 130,165.0 m<sup>3</sup> with a width of 75 m, a length of 204 m, and a height of 8.5 m. The view of the application building and NVS is given in Fig. 1.

The building has no extra heating, mechanical ventilation, or air conditioning unit. The heat requirement for the winter period is served by the local electrical heaters, whereas there is no cooling application for the summer period. The cooling needs in the summer period and the ventilation need in both the summer and winter period are just served by the NPV system. The NVS was placed on the roof of the building to provide ventilation through the stack effect since it was designed to remove the waste gases that occurred during the production processes.

The NVS has a structure consisting of sheet metal to withstand the high wind loads and external physical effects. The schematic illustration of the designed NPV is given in Fig. 2. In the constructed NVS, the sizes of a, c, L, and  $\beta$  are 0.50 m, 0.35 m, 6 m, and 110°, respectively.

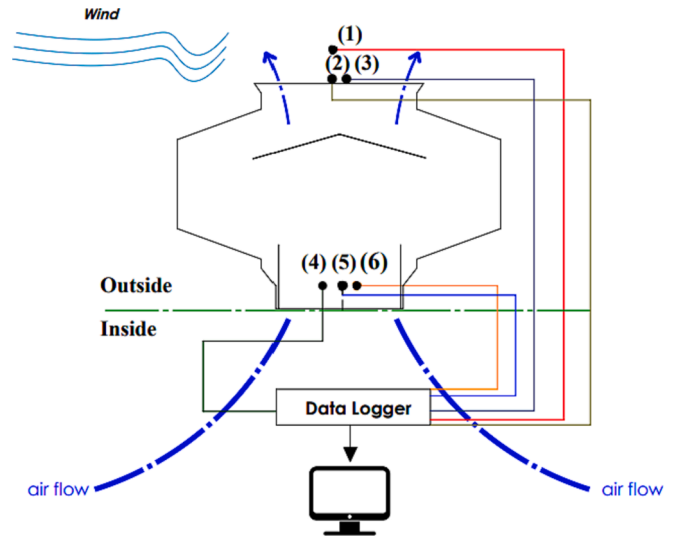


Fig. 3. The schematic of the experimental set-up.

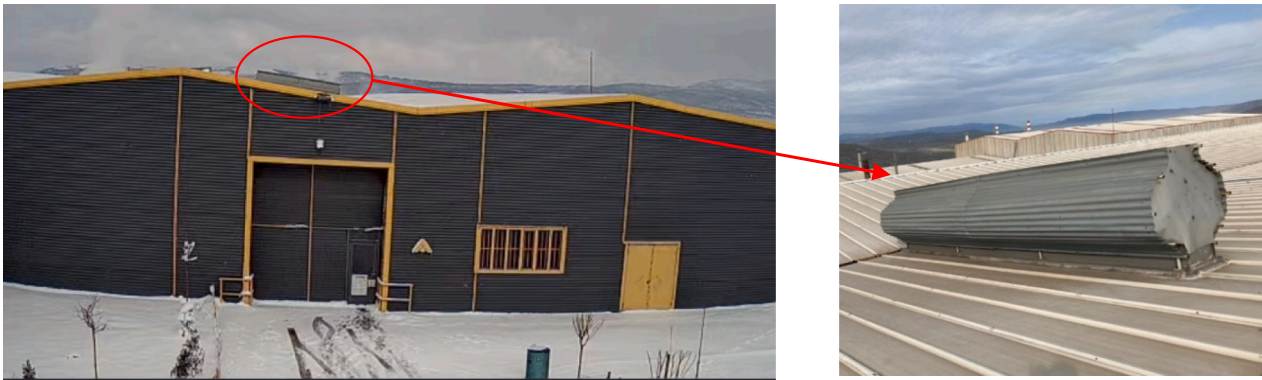


Fig. 1. The view of the application building and NVS.

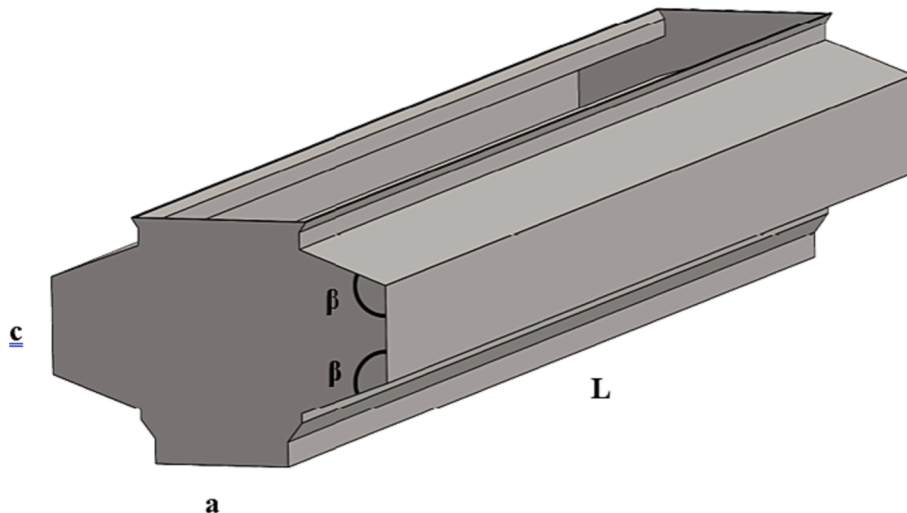


Fig. 2. Schematic illustration (solid model) of the designed NVS.

**Table 1**  
Experimental equipment and accuracy values [23].

Parameter	Point	Equipment	Sensitivity
T (°C)	3 and 6	ThermokotecBoynet T	±0.1
$v_r$ (m/s)	1	Delta Ohm HD 53.D	±0.03
$\varphi$ (%)	4	EMS ST-3XX	±1
P (Pa)	2 and 5	AKT-DPT2500-R8	±1

**Table 2**  
Uncertainty values of experimental parameters.

	$T_{in}$ (°C)	$T_{out}$ (°C)	$P_{in}$ (Pa)	$P_{out}$ (Pa)	$\varphi$ (%)	$v_r$ (m/s)
U	0.069	0.103	0.0007	0.0074	0.150	0.017

*Experimental set-up*

The working principle of the NVS is based on the combined effects of the thermal buoyancy-induced and wind-induced forces. For the determination of this combined effect, the experimental set-up was installed to measure the wind velocity ( $v_r$ ; point 1), outdoor temperature ( $T_{out}$ ; point 2), outdoor pressure ( $P_{out}$ ; point 3), relative humidity ( $\varphi$ ; point 4), indoor temperature ( $T_{in}$ ; point 5) and indoor pressure ( $P_{in}$ ; point 6) as given in Fig. 3.

A data logger recorded the measured values on an hourly basis. The properties of the used equipment are given in Table 1.

The reliability of the experimental set-up was validated by uncertainty analysis based on the measured data ( $X_m$ ) [24]. According to this analysis, the standard deviation (SD) is given as:

$$SD = \sqrt{\frac{\sum_{m=1}^n (X_m - \bar{X})^2}{n - 1}} \tag{1}$$

where  $\bar{X}$  is the average of the measured values calculated as:

$$\bar{X} = \frac{\sum X_m}{n} \tag{2}$$

The uncertainty (U) of the experimental data is defined as:

$$U = \frac{SD}{\sqrt{n}} \tag{3}$$

The results of the uncertainty analysis for each measured parameter are given in Table 2. According to the results, the uncertainties of the experiments are at an acceptable level.

*Determination of the ventilation rate*

The total ventilation rate ( $Q_T$ ) is defined as [25]:

$$Q_T = \sqrt{Q_r^2 + Q_{\Delta T}^2} \tag{4}$$

where  $Q_r$  is the wind-induced term that includes the ventilation occurred by the pressure difference depending on the change in wind velocity.  $Q_{\Delta T}$  is the thermal buoyancy-induced term that includes the ventilation occurred by the density change depending on the temperature difference. These two terms are given as [25,26]:

$$Q_r = C_d \cdot A_c \cdot \sqrt{\frac{2 \cdot \Delta P}{\rho_a}} \tag{5}$$

$$Q_{\Delta T} = C_d \cdot A_c \cdot \sqrt{2 \cdot g \cdot h \cdot \frac{T_{in} - T_{out}}{T_{in}}} \tag{6}$$

where  $A_c$  is the cross-sectional area of the opening of the NVS, and  $\rho_a$  is the density of moist air.  $T_{in}$  is the indoor temperature, and  $T_{out}$  is the outdoor temperature.  $\Delta P$  is the pressure difference between indoor (inlet opening) and outdoor (outlet opening), and  $h$  is the height of the NVS.  $C_d$  is the discharge coefficient and is given by [27]:

$$C_d = 0.0835 \cdot \left(\frac{T_{in} - T_{out}}{T_{in}}\right)^{(-0.313)} \tag{7}$$

*Energy and exergy analysis*

The energy and exergy analysis is based on the experimental measurements in this study. As a result of the hourly measurement period,

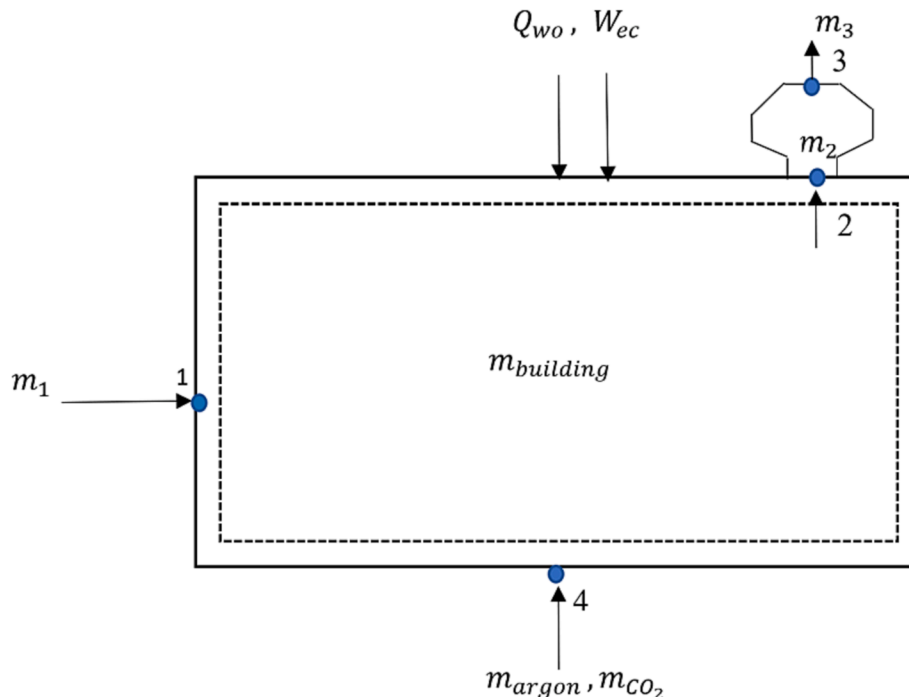


Fig. 4. Physical model of the ventilation system.

8760 measurements were recorded annually. With this, the balance equations were established for the control volumes under unsteady conditions. In this aim, the physical model for the ventilation of the space is conducted as given in Fig. 4.

The mass balance equation is constructed considering replacing the ventilated volume (point 2) with the fresh air from the outdoor (point 1). According to this, the mass balance is given by:

$$\overbrace{\rho_{a,1} \cdot \dot{Q}_T}^{m_1} + m_4 - \overbrace{\rho_{a,2} \cdot \dot{Q}_T}^{m_2} = \overbrace{V_{building} \cdot \rho_{a,building,t+\Delta t}}^{m_{sys,t+\Delta t}} - \overbrace{V_{building} \cdot \rho_{a,building,t}}^{m_{sys,t}} \quad (8)$$

Here  $m_4$  indicates the sum of the mass of welding gases. The welding gasses used in the production process are argon ( $m_{argon}$ ) and CO<sub>2</sub> ( $m_{CO_2}$ ). Welding gas consumptions were added to the calculations considering the annual data of Ref [23]. The working activity in the building (between 08:30 am and 5:30 pm, six days a week) was also considered in the study. In this regard,  $m_4$  was introduced as zero (0) to calculations when there is no operational activity in the building.  $\rho_{a,1}$  and  $\rho_{a,2}$  were the average values for the measurement range ( $\Delta t$ ). Since the balances were constructed on experimental data, the measurement range ( $\Delta t$ ) in balance equations was 1 h. Also, the density of the building air was assumed to be equal to point 2 ( $\rho_{a,building,t} = \rho_{a,2,t}$ ) at the particular measured time of  $t$ . Accordingly, the energy balance is given by:

$$\begin{aligned} Q_L = E_{sys,t+\Delta t} - E_{sys,t} - (m_2 \cdot h_2) - (m_1 \cdot h_1) - (m_{argon} \cdot h_{argon}) \\ - (m_{CO_2} \cdot h_{CO_2}) - (W_{ec}) - (Q_{wo}) \end{aligned} \quad (9)$$

where  $W_{ec}$  and  $Q_{wo}$  are the electricity consumption and the heat load occurred by the workers, respectively. Theof the electricity consumption and heat loads were taken from the hourly recorded data by the industrial company in question [23]. The energy of the system at a measured time of  $t$  is given as:

$$E_{sys,t} = m_{sys,t} \cdot U_{sys,t} \quad (10)$$

where  $U_{sys,t}$  is the internal energy of the building system. For the constant volume, it is given as:

$$U_{sys,t} = C_{v,sys} \cdot T_t \quad (11)$$

The specific heat ( $C_{v,sys}$ ) can be obtained as follows;

$$C_{v,sys} = C_{p,sys} - R_{sys} = \frac{h_{sys,t}}{T_t} - R_{sys} \quad (12)$$

where  $R_{sys}$  is the gas constant and  $h_{sys,t}$  is the enthalpy of the system at the measured time of  $t$  obtained as follows:

$$h_{sys,t} = \frac{m_{CO_2,t} \cdot h_{CO_2,t} + m_{argon,t} \cdot h_{argon,t} + m_{air,t} \cdot h_{air,t}}{m_{CO_2,t} + m_{argon,t} + m_{air,t}} \quad (13)$$

$$R_{sys,t} = \frac{R_u}{\frac{1}{m_{total,t}} (m_{CO_2,t} + m_{argon,t} + m_{air,t})} \quad (14)$$

where  $R_u$  is the universal gas constant, and  $m_{total}$  is the total mass of the building environment.  $m_{CO_2,t}$ ,  $m_{argon,t}$ ,  $m_{air,t}$  are the hourly mass rate of CO<sub>2</sub>, argon, and moist air, respectively.  $h_{CO_2,t}$ ,  $h_{argon,t}$ ,  $h_{air,t}$  are the hourly average CO<sub>2</sub>, argon, and moist air enthalpy, respectively. When there is no operational activity in the building,  $m_{CO_2,t}$ ,  $m_{argon,t}$ ,  $m_{air,t}$  are equal to zero (0). For the active working period, these values are calculated by [28]:

$$h_{air,t} = 1.006 \cdot T_t + \omega_{air} (1.86 \cdot T_t + 2501) \quad (15)$$

$$h_{CO_2,t} = 7.94 \cdot T_t^4 - 33.69 \cdot 10^{-6} \cdot T_t^3 + 55.18 \cdot 10^{-3} \cdot T_t^2 + 24.99 \cdot T_t - \left( \frac{0.136 \cdot 10^6}{T_t} \right) \quad (16)$$

$$\begin{aligned} h_{argon,t} = 1.09 \cdot 10^{-8} \cdot T_t^4 - 1.46 \cdot 10^{-7} \cdot T_t^3 + 2.87 \cdot 10^{-7} \cdot T_t^2 \\ + 20.78 \cdot T_t - \left( \frac{3.661 \cdot 10^{-8}}{T_t} \right) \end{aligned} \quad (17)$$

Here  $T_t$  is the supply temperature, equal to the indoor temperature. Finally, the exergy balance of the system is given by:

$$Ex_{in} - Ex_{out} - Ex_d - Ex_Q + Ex_W + Ex_{wo} = Ex_{sys,t+\Delta t} - Ex_{sys,t} \quad (18)$$

where  $Ex_{in}$  and  $Ex_{out}$  are the inlet and outlet exergy of the flows, respectively.  $Ex_d$  is the destructed exergy,  $Ex_Q$  is the exergy due to the heat loads,  $Ex_W$  is the work (electricity) exergy,  $Ex_{wo}$  is the labour exergy,  $Ex_{sys,t}$  is the exergy of the system at the measured time of  $t$ . Since there is no chemical reaction during the welding process, the chemical exergies were not included. According to this, the exergy of the flow is given as:

$$Ex_{in} = \overbrace{Ex_{air}}^{point1} + \overbrace{Ex_{argon} + Ex_{CO_2}}^{point4} \quad (19)$$

$$Ex_{out} = \overbrace{Ex_{air} + Ex_{argon} + Ex_{CO_2}}^{point2} \quad (20)$$

Here  $Ex_{air}$ ,  $Ex_{argon}$  and  $Ex_{CO_2}$  are the exergy of the air and gases used in the welding process. These exergy terms are given as [29]:

$$\begin{aligned} Ex_{air} = m_{air} \cdot (C_{p,air} + \omega_{air} \cdot C_{vair}) \cdot T_0 \cdot \left[ \left( \frac{T_{in,t}}{T_0} \right) - 1 - \ln \left( \frac{T_{in,t}}{T_0} \right) \right] \\ + (1 + 1.6078 \cdot \omega_{air}) \cdot R_a \cdot T_0 \cdot \ln \left( \frac{P_{in,t}}{P_0} \right) \\ + R_a \cdot T_0 \cdot \left\{ \frac{1 + 1.6078 \cdot \ln((1 + 1.6078) \cdot \omega_0)}{(1 + 1.6078 \cdot \omega_{air}) + 1.6078 \cdot \omega_{sys,t} \cdot \ln \left( \frac{\omega_{air}}{\omega_0} \right)} \right\} \end{aligned} \quad (21)$$

$$Ex_{argon} = m_{argon} \cdot C_{p,argon} \left( T_t - T_0 - T_0 \cdot \ln \left( \frac{T_{ws}}{T_{in}} \right) \right) + R_{argon} \cdot T_0 \cdot \ln \left( \frac{P_t}{P_{atm}} \right) \quad (22)$$

$$Ex_{CO_2} = m_{CO_2} \cdot C_{p,CO_2} \left( T_t - T_0 - T_0 \cdot \ln \left( \frac{T_{in}}{T_{in}} \right) \right) + R_{argon} \cdot T_0 \cdot \ln \left( \frac{P_t}{P_{atm}} \right) \quad (23)$$

where  $R_{argon}$  is the gas constant of argon (0.208 kJ/kgK) and  $R_{CO_2}$  is the gas constant of CO<sub>2</sub> (0.188 kJ/kgK). The exergy of the system is given by:

$$\begin{aligned} Ex_{sys,t} = m_{sys,t} \cdot (C_{p,sys,t} + \omega_{sys,t} \cdot C_{v,sys,t}) \cdot T_0 \cdot \left[ \left( \frac{T_{in,t}}{T_0} \right) - 1 - \ln \left( \frac{T_{in,t}}{T_0} \right) \right] \\ + (1 + 1.6078 \cdot \omega_{sys,t}) \cdot R_a \cdot T_0 \cdot \ln \left( \frac{P_{in,t}}{P_0} \right) \\ + R_a \cdot T_0 \cdot \left\{ \frac{1 + 1.6078 \cdot \ln((1 + 1.6078) \cdot \omega_0)}{(1 + 1.6078 \cdot \omega_{sys,t}) + 1.6078 \cdot \omega_{sys,t} \cdot \ln \left( \frac{\omega_{sys,t}}{\omega_0} \right)} \right\} \end{aligned} \quad (24)$$

with

$$\omega_{sys,t} = \frac{0.622 \cdot \varphi \cdot P_{sat,T}}{P_2 - \varphi \cdot P_{sat,T}} \quad (25)$$

$Ex_{ec}$ ,  $Ex_{wo}$  are the exergy of electric consumption of the building and the exergy of workers, respectively:

$$Ex_{ec} = W_{ec} \quad (26)$$

$$Ex_{wo} = n_{wo} \cdot 280 \quad (27)$$

Here,  $n_{wo}$  is the number of workers in the building and taken as 15 people. The exergy efficiency of the system is given by:

**Table 3.T**  
He emissions of the ng combustion[33,34].

Fuel	Emission			
	CO <sub>2</sub>	CO	NO <sub>2</sub>	SO <sub>2</sub>
NG*	1.95023	0.00024	0.03384	-

\*per kmole-fuel.

$$\epsilon = 1 - \frac{Ex_d}{Ex_{in}} \quad (28)$$

*Economic and environmental evaluation*

For the economic evaluation, net present values (NPV) analysis was handled since it considers the time value of the money for the lifecycle of

the system. NPV is defined as [30,31]:

$$NPV = \sum_{t=0}^n \left( \frac{1}{(1+r)^t} \right)^{TVM} C_{cf} - C_i \quad (29)$$

where  $C_{cf}$  is the cash flow,  $C_i$  is the investment cost,  $r$  is the discount rate of 14.75% [32], and  $t$  is the related year of the system’s lifetime. TVM is the multiplier that explains the time value of the money in NPV analysis. When  $t = 0$ , it explains the present time values that the system is constructed. The lifetime of the system ( $n$ ) was assumed as 20 years. The investment cost includes the cost of pipe ( $C_p$ ), galvanized sheet ( $C_{st}$ ), labour cost ( $C_L$ ), and assembly cost ( $C_a$ ). The initial investment cost, considering the salvage cost ( $C_s$ ) of the system at the end of the lifetime, is given as follows:

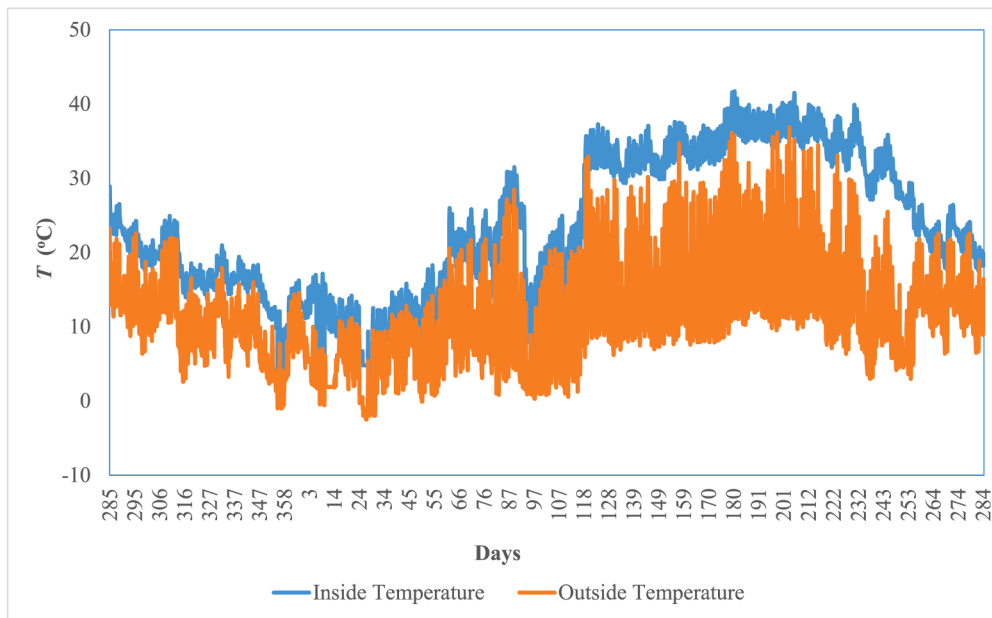


**Fig. 5.** The variation of inside ( $T_{in}$ ) and outside ( $T_{out}$ ) temperatures.

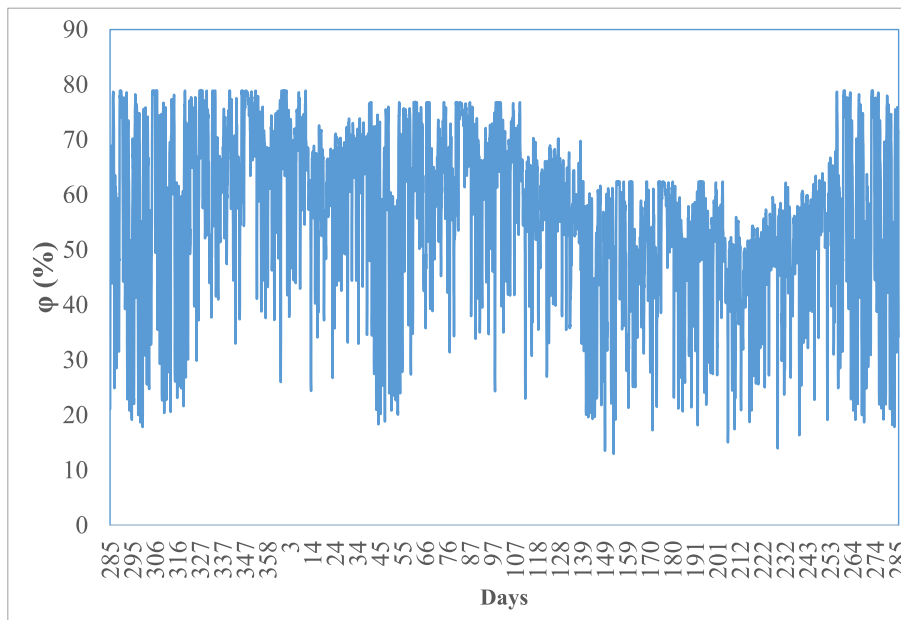


**Fig. 6.** The variation of relative humidity ( $\phi$ ).

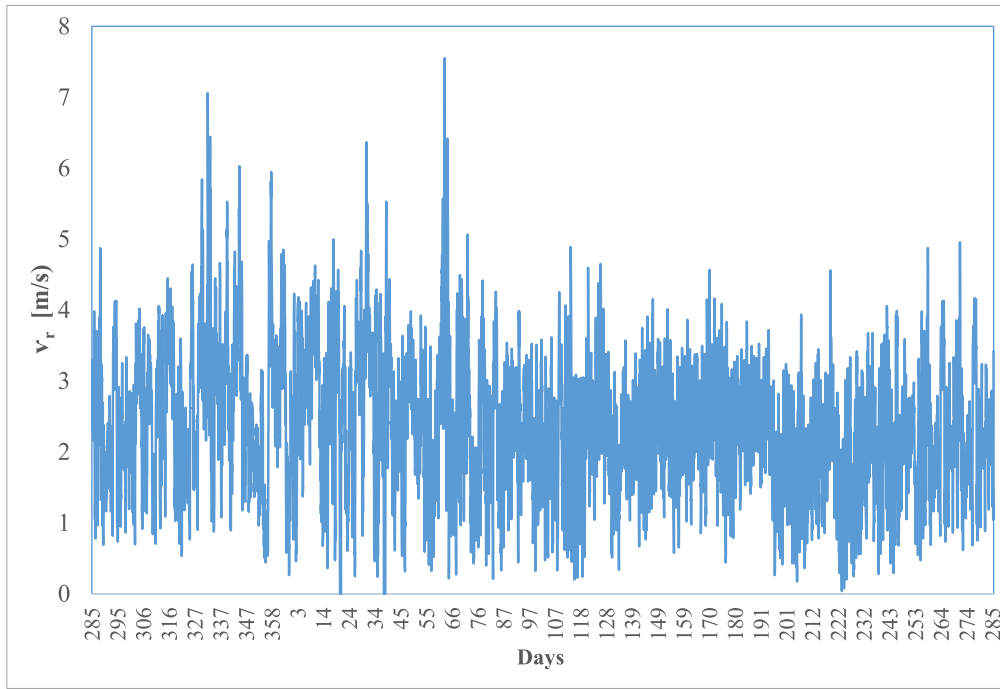


Fig. 7. The variation of wind velocity ( $v_r$ ).

$$C_i = C_p + C_{st} + C_L + C_a - C_s \tag{30}$$

$C_s$  is the 10 % sum of the other investment terms [31]. The annual cash flow was obtained considering a mechanical ventilator system instead of the NVS. For an annual working time of 8760 h, the cash flow is defined as:

$$C_{cf} = W_e \cdot f_e \cdot 8760 \tag{31}$$

Here  $W_e$  is the required power of the fan, and  $f_e$  is unit electricity price. The saved electricity via NVS also means a saving in natural gas (NG)

consumption since the company’s electricity requirement is supplied by NG sourced power plant. The annual savings of NG (in kmole) is given by:

$$n_{NG} = \frac{W_e \cdot 8760}{HV \cdot \eta_{te}} \tag{32}$$

Here  $HV$  is the heating value (38330 kJ/h), and  $\eta_{te}$  is the efficiency of the power plant (38%). The saved NG also would decrease the emissions sourced by the combustion of NG in the power plant. The emissions that occurred by NG combustion are given in Table 3 [33,34].

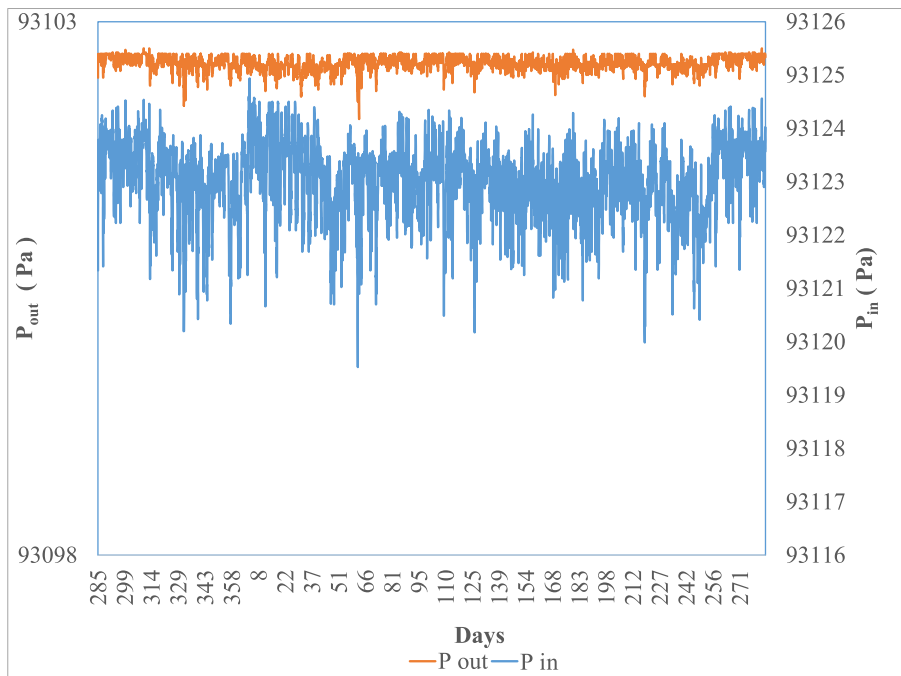


Fig. 8. The variation of  $P_{in}$  and  $P_{out}$ .

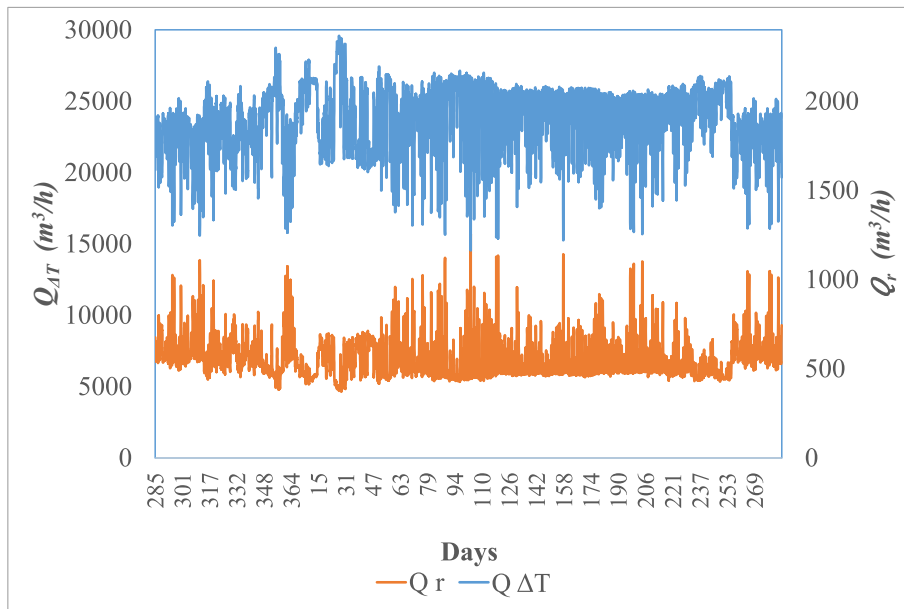


Fig. 9. The variation of  $Q_r$  and  $Q_{\Delta T}$ .

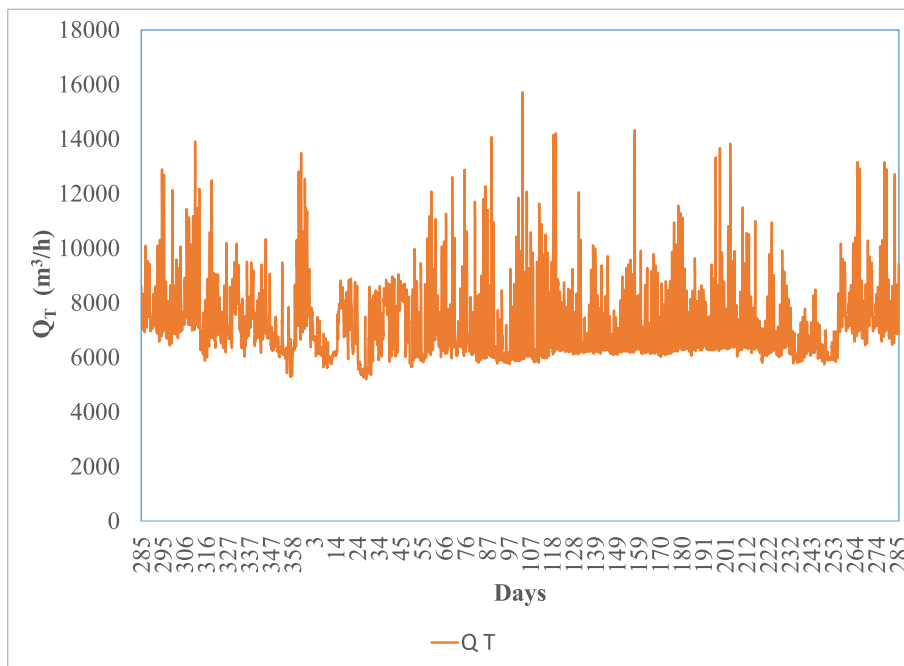


Fig. 10. The variation of  $Q_T$ .

**Results and discussion**

The time-dependent variation of the inside ( $T_{in}$ ) and outside ( $T_{out}$ ) temperature values are shown in Fig. 5 for one year. Fluctuations in graph slopes manifest the effect of seasonal events on outside and inside temperatures.

According to Fig. 5, the outside temperature values vary between  $-3\text{ }^{\circ}\text{C}$  and  $36\text{ }^{\circ}\text{C}$  depending on the climatic factors of the region where the building is located. The interior temperature values vary between  $3\text{ }^{\circ}\text{C}$  and  $40\text{ }^{\circ}\text{C}$  depending on the physical factors of working inside the building and the outdoor climatic effects. According to the measurements, the temperature-induced (buoyancy effect) for ventilation is available for the year, making the NVS suitable. The measurements of

effective parameters of relative humidity ( $\varphi$ ) and wind velocity ( $v_r$ ) were also obtained. The variation of  $\varphi$  and  $v_r$  are given in Fig. 6 and Fig. 7, respectively.

According to Fig. 6, the relative humidity varies between 10% and 80% during the year. The main reason for the change in relative humidity is the climatic changes, labour effects and external geographical factors of the building.

According to Fig. 7,  $v_r$  reach up to 7.6 m/s. The highest wind velocity was observed on the 66th day of the year. The indoor ( $P_{in}$ ) and outdoor ( $P_{out}$ ) pressures were also measured to determine the ventilation rate. Fig. 8 shows the variation of  $P_{in}$  and  $P_{out}$ .

According to Fig. 8, the indoor pressure varies between 93116 Pa and 93118 Pa, whereas the outdoor pressure varies between 93118 Pa and

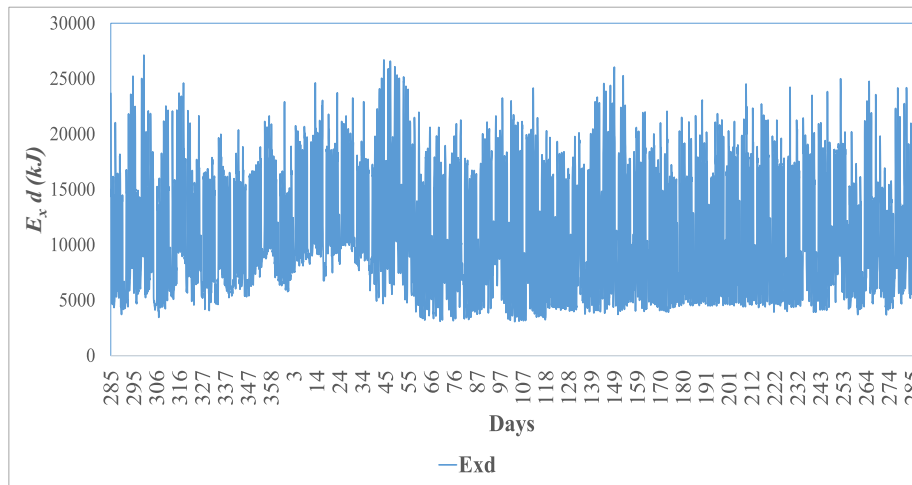


Fig. 11. The variation of exergy destruction rate ( $Ex_d$ ).

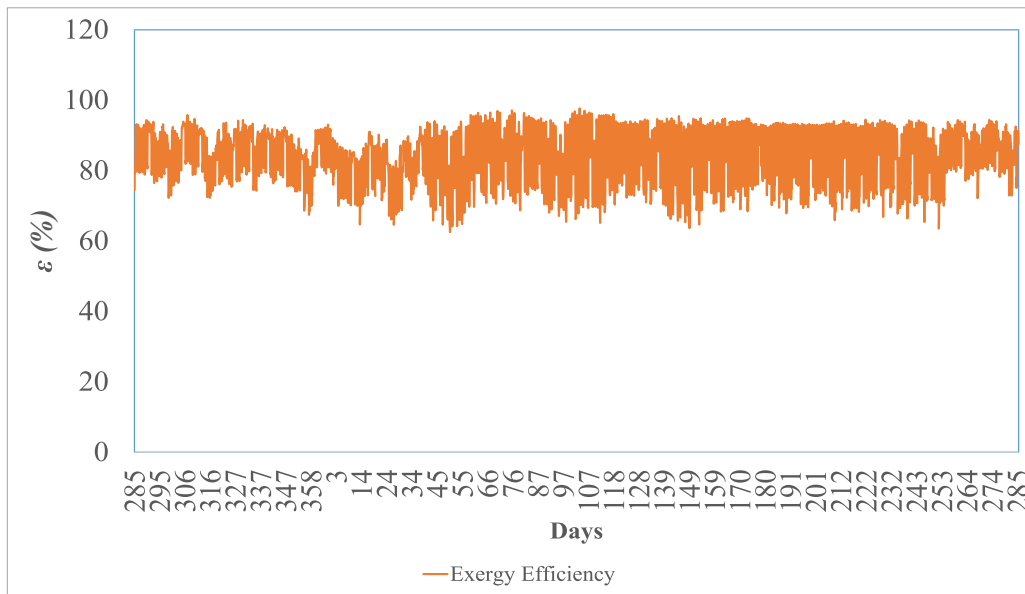


Fig. 12. The variation of exergy efficiency ( $\epsilon$ ).

93125 Pa. According to the measurement results, the wind-induced effects are also available all year round. So, the temperature-induced ( $Q_{\Delta T}$ ), wind-induced ventilation ( $Q_r$ ), and total ventilation ( $Q_T$ ) rates were calculated. The variation of  $Q_{\Delta T}$  and  $Q_r$  is given in Fig. 9, whereas the variation of  $Q_T$  is given in Fig. 10.

According to Fig. 10, the maximum ventilation rate was observed as  $15,728.8 \text{ m}^3/\text{h}$  on the 107th day of the year in the winter season. In this case,  $T_{in}$ ,  $T_{out}$ ,  $v_r$ ,  $\phi$ , and  $\Delta P$  were recorded as  $20.20 \text{ }^\circ\text{C}$ ,  $20.95 \text{ }^\circ\text{C}$ ,  $2.18 \text{ m/s}$ ,  $66.05\%$ , and  $21.18 \text{ Pa}$ , respectively. The minimum ventilation rate was  $5201.8 \text{ m}^3/\text{h}$  on the 27th day of the year in winter. In this case,  $T_{in}$ ,  $T_{out}$ ,  $v_r$ ,  $\phi$ , and  $\Delta P$  were recorded as  $-1.91 \text{ }^\circ\text{C}$ ,  $4.0 \text{ }^\circ\text{C}$ ,  $2.52 \text{ m/s}$ ,  $69.53\%$ , and  $20.05 \text{ Pa}$ , respectively. The average ventilation rate was recorded as  $7060.7 \text{ m}^3/\text{h}$  for a yearlong time. Under these circumstances, the time-stepped exergy analyses were conducted. The results are given in Fig. 11 for the exergy destruction rate ( $Ex_d$ ) and Fig. 12 for the exergy efficiency ( $\epsilon$ ).

According to Fig. 11, the maximum exergy destruction rate was recorded as  $27,124.81 \text{ kJ}$  on the 300th day of the year in the winter season. In this case,  $T_{in}$ ,  $T_{out}$ ,  $v_r$ ,  $\phi$ , and  $\Delta P$  were recorded as  $17.32 \text{ }^\circ\text{C}$ ,  $20.78 \text{ }^\circ\text{C}$ ,  $1.74 \text{ m/s}$ ,  $17.0\%$ , and  $21.42 \text{ Pa}$ , respectively. The minimum

exergy destruction was recorded as  $3,066.78 \text{ kJ}$  on the 104th day of the year in the winter season. In this case,  $T_{in}$ ,  $T_{out}$ ,  $v_r$ ,  $\phi$ , and  $\Delta P$  were recorded as  $20.20 \text{ }^\circ\text{C}$ ,  $20.95 \text{ }^\circ\text{C}$ ,  $2.18 \text{ m/s}$ ,  $66.05\%$ , and  $21.18 \text{ Pa}$ , respectively. According to Fig. 12, the exergy efficiency of the system was recorded ranging between  $65\%$  and  $95\%$ .

The total volume of the ventilated building ( $V_b$ ) is  $130,165.0 \text{ m}^3$  which means a required ventilation rate for removing the non-breathable gases occurred due to the manufacturing processes. The required NVS number ( $N_{required-NVS}$ ) for homogeneous ventilation of the complete building volume is 26, considering the minimum ventilation rate ( $5201.8 \text{ m}^3/\text{h}$ ). The required ventilation rate at the minimal extreme points could be achieved for a continuous ventilating process. Economic parameters for NPV analysis were determined considering this extreme point. The results of the NPV analysis are given in Table 4.

In NPV analysis, the benefits were determined considering the mechanical ventilation requirements for the exact parameters of NVS. In this case, the required power was determined as  $4 \text{ kW}$  whereas the annual benefit was calculated as  $6,678.52 \text{ \$}$  with the information of the electricity price of  $0.19 \text{ \$/kWh}$ . Finally, the NPV value of the system was determined as  $18,576.61 \text{ \$}$ , which means that the designed NVS is

**Table 4**  
The results of economic evaluation (in \$).

	Years				
	Present	5	10	15	20
<b>Investment</b>					
Piping ( $C_p$ )	-6,723.02				
Sheet Metal ( $C_{st}$ )	-6,990.70				
Welding ( $C_w$ )	-5,565.81				
Labour ( $C_l$ )	-2,236.34				
Assembly ( $C_a$ )	-4,440.65				
Total	-25,556.55				
<b>Cash flow</b>					
Operating and Maintenance		-127.78	-127.78	-127.78	-127.78
Benefit from electricity saving		6,678.52	6,678.52	6,678.52	6,678.52
Salvage ( $C_s$ )	2,555.65	0.00	0.00	0.00	0.00
Total Cash Flow	-25,556.55	6,550.74	6,550.74	6,550.74	6,550.74
TVM (with $r = 14.75\%$ )	1.00	0.50	0.25	0.13	0.06
The Cumulative Cash Flow	-23,000.90	9,752.80	42,506.50	75,260.20	108,013.90
Present value	-23,000.90	3,292.51	1,654.87	831.76	418.06
<b>NPV</b>	<b>18,576.61</b>				

1 US\$=15.44 ₺.

**Table 5**  
The results of environmental evaluation.

Saving	Unit	Yearly basis	Lifecycle basis
Natural Gas	m <sup>3</sup>	12,092.20	241,844.0
Electricity	GWh	0.0345	0.690
CO <sub>2</sub>	ton	1045.11	20,902.20
CO	ton	0.127	2.541
NO <sub>2</sub>	ton	18.26	365.36
NO	ton	4.57	91.51

profitable for industrial buildings. The saved emissions were determined based on the saved electricity obtained from the NG-fueled plant, as given in Table 5.

According to Table 5, saving an NG in the amount of 241,844.0 during the system lifetime of 20 years is possible. This saving also means avoidance of 20,902.20 tones of CO<sub>2</sub>, 2.541 tones of CO, 365.36 tones of NO<sub>2</sub>, and 91.51 tones of NO.

## Conclusion

In this study, the natural ventilation of an industrial building was investigated via a newly designed stack-type ventilation system (NVS). The NSV was designed and constructed for the disposal of the welding gases to obtain suitable working conditions. The designed NVS was experimentally investigated yearly to view the ventilation capability for both the winter and summer conditions. Time-stepped exergy analyses were performed based on the experimental values on an hourly basis. So, the exergy destructions, as well as the exergy efficiency, were determined since the destructions (without any power consumption means) generated entropy by the disposal of unbreathable gases. The economic evaluation of the system via the net present value (NPV) method was conducted to view the invisibility of the NVS. Finally, the environmental evaluation was compared to the mechanical ventilation case for the exact requirements. The designed NVS was found as capable of the ventilation of an industrial building since it provides continuous ventilation for all winter and summer conditions. The minimum exergy efficiency was determined as 65 % whereas the maximum was obtained as 95%. The higher exergy efficiency ratios designate the lower entropy generations in the environment which could be attributed as pretty much environment-friendly system in comparison to mechanical ventilation systems with power consumption. For the investigated building with a volume of 130,165.0 m<sup>3</sup>, the required number of NVS was determined as 26 for the disposal of the non-breathable gases that

occurred during the manufacturing process. Under these circumstances, the designed NVS was found as profitable with an NPV of 18,576.61 \$. Also, it is available to save consumption of natural gas of 241,844.0 m<sup>3</sup> since there is no power consumption. From the environmental point of view, it means a saving of CO<sub>2</sub> of 20,902.20 tones.

The handled NVS system was designed to observe the ventilation effects of the system for an industrial building. The system sizes were randomly selected appropriate to the building's roof structure. Therefore, the size of the system needs to be optimized. The authors currently handle the studies on the optimization of the NVS within the scope of the ongoing Ph.D. dissertation.

Declaration of interests.

Onur Kayapinar has patent licensed to 2019–08313.

## CRediT authorship contribution statement

**Onur Kayapinar:** Data curation, Investigation, Methodology, Validation. **Oğuz Arslan:** Conceptualization, Methodology, Validation, Investigation.

## Declaration of Competing Interest

The authors declare that they have no known competing financial interests or personal relationships that could have appeared to influence the work reported in this paper.

## Data availability

No data was used for the research described in the article.

## References

- [1] Y. Li, P. Heiselberg, Analysis methods for natural and hybrid ventilation - a critical literature review and recent developments, *Int. J. Vent.* 1 (4) (2003) 3–20.
- [2] D. Han, S. Kim, J.H. Choi, Y.S. Kim, H.S. Chung, H. Jeong, N. Watjanatopin, C. Ruangpattanawit, S.H. Choi, Experimental study on thermal buoyancy-induced natural ventilation, *Energ. Build.* 177 (2018) 1–11.
- [3] Y.S. Kim, H. Chung, H. Jeong, S.-K. Song, C. Yi, S.-H. Choi, Experimental study on a fixed type natural ventilator, *Int. J. Air-Cond. Refrig. 24* (03) (2016) 1650016.
- [4] D. Costala, B. Blocken, M. Hensen, Over of pressure coefficient data in building energy simulation, *Build. Environ.* 44 (2009) 2027–2036.
- [5] Y. Li, A. Delsante, Natural ventilation induced by combined wind and thermal forces, *J. Build. Environ.* 36 (1) (2001) 59–71.
- [6] W. Li, Q. Chen, Design-based natural ventilation cooling potential evaluation for buildings in China, *J. Build. Eng.* 41 (2021) 102345.

- [7] K. Espinoza, A. López, D.L. Valera, F.D. Molina-Aiz, J.A. Torres, A. Peña, Effects of ventilator configuration on the flow pattern of a naturally ventilated three-span Mediterranean greenhouse, *Biosyst. Eng.* 164 (2017) 13–30.
- [8] S. Hulsure, R.S. Maurya, Numerical investigation of wind driven natural ventilation in a mega warehouse building, *Int. J. Fluid Eng.* 23 (2019) 1–23.
- [9] M. Gil-Baez, A. Barrios-Padura, M. Molina-Huelva, R. Chacartegui, Natural ventilation systems in 21st-century for near zero energy school buildings, *Energy* 137 (2017) 1186–1200.
- [10] A. Mukhtar, M.Z. Yusoff, K.C. Ng, The potential influence of building optimization and passive design strategies on natural ventilation systems in underground buildings: the state of the art, *Tunn. Undergr. Space Technol.* 92 (2019) 103065.
- [11] P.V. Dorizas, S. Samuel, M. Dejan, Y. Keqin, M.M. Dimitris, L. Tom, Performance of a natural ventilation system with heat recovery in UK classrooms: an experimental study, *Energ. Build.* 179 (2018) 278–291.
- [12] X. Su, X.u. Zhang, J. Gao, Evaluation method of natural ventilation system based on thermal comfort in China, *Energ. Build.* 41 (1) (2009) 67–70.
- [13] D. Shi, Y. Gao, P. Zeng, B. Li, P. Shen, C. Zhuang, Climate adaptive optimization of green roofs and natural night ventilation for lifespan energy performance improvement in office buildings, *Build. Environ.* 223 (2022) 109505.
- [14] Y. Chen, J. Gao, J. Yang, U. Berardi, G. Cui, An hour-ahead predictive control strategy for maximizing natural ventilation in passive buildings based on weather forecasting, *Appl. Energy* 333 (2023) 120613.
- [15] Z.M. Gilvaei, A.H. Poshtiri, A.M. Akbarpoor, A novel passive system for providing natural ventilation and passive cooling: evaluating thermal comfort and building energy, *Renew. Energy* 198 (2022) 463–483.
- [16] J. Shaeri, M. Mahdavinnejad, M.H. Pourghasemian, A new design to create natural ventilation in buildings: wind chimney, *J. Build. Eng.* 59 (2022) 105041.
- [17] G. Tognon, M. Marigo, M. De Carli, A. Zarrella, Mechanical, natural and hybrid ventilation systems in different building types: energy and indoor air quality analysis, *J. Build. Eng.* 76 (2023) 107060.
- [18] M. Xie, Y. Wang, Z. Liu, G. Zhang, Effect of the location pattern of rural residential buildings on natural ventilation in mountainous terrain of central China, *J. Clean. Prod.* 340 (2022) 130837.
- [19] X.X. Li, K.L. Huang, G.H. Feng, W.Y. Li, J.X. Wei, Night ventilation scheme optimization for an Ultra-low energy consumption building in Shenyang, China, *Energy Reports* 8 (2022) 8426–8436.
- [20] Y.i. He, Y. Chu, H. Zang, J. Zhao, Y. Song, Experimental and CFD study of ventilation performance enhanced by roof window and mechanical ventilation system with different design strategies, *Build. Environ.* 224 (2022) 109566.
- [21] J. Song, X. Huang, D. Shi, W.E. Lin, S. Fan, P.F. Linden, Natural ventilation in London: towards energy-efficient and healthy buildings, *Build. Environ.* 195 (2021) 107722.
- [22] S.N. Ma'bdeh, A. Al-Zghoul, T. Alradaideh, A. Bataineh, S. Ahmad, Simulation study for natural ventilation retrofitting techniques in educational classrooms – a case study, *Heliyon* 6 (10) (2020) e05171.
- [23] Kayapinar O. Using of Natural Ventilation System for Disposal of Breathable Gases in Production Lines and Improving Indoor Air Quality, Ph.D. Dissertation, Institute of Applied Sciences, Bilecik Seyh Edebali University, 2023 (on going).
- [24] H. Arat, O. Arslan, U. Ercetin, A. Akbulut, Experimental study on heat transfer characteristics of closed thermosyphon at different volumes and inclination angles for variable vacuum pressures, *Case Stud. Thermal Eng.* 26 (2021) 101117.
- [25] Engineering Guide: Natural Ventilation, Section K. Price Industries, 2011. Available from: <https://www.priceindustries.com/content/uploads/assets/literature/engineering-guides/natural-ventilation-engineering-guide.pdf>.
- [26] A. Bhaitea, Natural ventilation principles and practices: HVAC e-Book, Createspace Independent Publishing Platform (2014).
- [27] S.B. Riffat, A study of heat and mass transfer through doorway in traditional built house, *ASHRAE Trans.* 95 (1989) 573–583.
- [28] NIST Chemistry Web-Book: NIST Standart Reference Database, Number 69, 2023. Available from: <http://webbook.nist.gov/chemistry>.
- [29] A. Hepbasli, A key review on exergetic analysis and assessment of renewable energy resources for a sustainable future, *Renew. Sustain. Energy Rev.* 12 (3) (2008) 593–661.
- [30] O. Arslan, A.E. Arslan, Performance evaluation and multi-criteria decision analysis of thermal energy storage integrated geothermal district heating system, *Process Saf. Environ. Prot.* 167 (2022) 21–33.
- [31] O. Arslan, D. Kilic, Concurrent optimization and 4E analysis of organic Rankine cycle power plant driven by parabolic trough collector for low-solar radiation zone, *Sustain. Energy Technol. Assess.* 46 (2021) 101230.
- [32] Central Bank of Republic of Turkey, Exchange and inflation rates, Available from: <https://tcmb.gov.tr>. Last access: May 27<sup>th</sup>, 2022.
- [33] O. Arslan, M.A. Ozgur, H.D. Yildizay, R. Kose, Fuel effects on optimum insulation thickness: an exergetic approach, *Energy Sources Part A* 32 (2009) 128–147.
- [34] O. Arslan, M. Ucar, Assessment of improvement potential of condensed combi boiler via advanced exergy analysis, *Therm. Sci. Eng. Progr.* 23 (2021), 100853.